Study of T11 Beam Specifications and Rate of Muon Energy Loss in the Caldet

Leo Jenner

12th June 2002

First Year Report

University College London

1 Abstract

By comparing Monte Carlo simulation of the interaction of positive muons in the calibration detector at CERN to real data, it has been possible to deduce some of the parameters of the beam. By studying the distance these muons are able to travel through the detector before being stopped, a discrepancy has been found between the way the Monte Carlo simulates the interactions compared to that actually seen. This is can be explained by a deviation of the beam characteristics from those stated by CERN: the spread of momenta of the particles in the beam is around 4.5% and not 1.5% and the peak of the actual momentum maximum of beam particles is around 4% higher than expected.

The observed rate of loss of energy of real muons as they travel through the detector fits the Monte Carlo simulations well.

2 Introduction

Neutrinos are amongst the most abundant particles in the universe, and yet there is still a great deal about them that is not well understood. It is not known whether neutrinos are stable, whether they have electromagnetic structure or even with certainty whether they have mass on not. Conversely, incredibly accurate data for electrons has been determined - for example the magnetic moment of the electron is known to one part in 10^{11} .

Two well documented phenomenon are cause for even further concern. The Solar Neutrino Problem is a discrepancy between the number of ν_e 's predicted by the Solar Model and those observed arriving at the earth from the sun. Helioseimological studies support the Solar Model, pushing the problem back to the realm of Particle Physics. In addition, the expected ratio of ν_μ to ν_e of 2:1 arriving at the surface of the earth from cosmic ray interactions in the upper atmosphere, is not observed.

This evidence points to the conclusion that the neutrino may not operate within the confines of the Standard Model of Particle Physics, as it is stands today. This is a disturbing prospect since the Standard Model is so successful in many other areas of particle physics. But it also makes the study of neutrino physics an exciting field of contemporary research.

3 Neutrino Oscillations

One of the more favoured theories to explain the observed events is that first suggested by Pontecorvo in 1967; neutrino oscillations. In nature it is observed and is now well understood that the allowed mass eigenstates of quarks are not the same as their allowed weak eigenstates. A weak force carrying particle 'sees' a quark as a mixture of all three generations. This allows the weak force to change quarks from one generation to another.

By simply extending this principle to the lepton sector, a scenario can be arrived at where neutrinos of one type can change into another. The consequence of this is that neutrinos should have a definite mass, although maybe very small.

Neutrinos were thought to be massless within the Standard Model. They seemed to travel at the speed of light which precludes them from having any mass. Furthermore, a strange quirk of the weak force allows only 'left-handed' particles to interact. Massive neutrinos can be flipped to a 'right-handed' state where interactions with matter cease being possible.

But massive neutrinos also help in other areas. They contribute mass to the universe, reducing the huge discrepancy between observed gravitational effects and the detectable matter that should be causing them.

A description of the relationship between the mass and weak eigenstates of neutrinos can be given by a 3 x 3 matrix, rather like the Cabibbo-Kobayashi-Maskawa

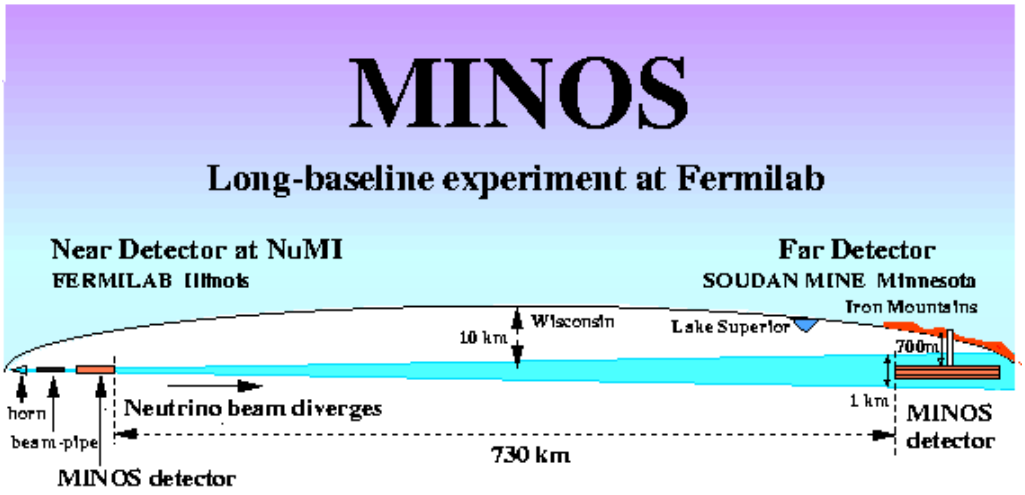

Figure 1: Minos experiment baseline

representation for quarks. However a two flavour approximation is much simpler and adequate for most instances:

$$\begin{bmatrix} \nu_\alpha \\ \nu_\beta \end{bmatrix} = \begin{bmatrix} \cos\theta & \sin\theta \\ -\sin\theta & \cos\theta \end{bmatrix} \begin{bmatrix} \nu_1 \\ \nu_2 \end{bmatrix}$$

which gives the transition probability equation for flavour α to flavour β :

$$P_{\alpha\beta} = sin^2 2\theta sin^2(1.27\Delta m^2 L/E_\nu)$$

where θ is the neutrino mixing angle, $\Delta m^2 = m_1^2$ - m_2^2 of mass eigenstate 1 and 2, L is the path length in km and E is the neutrino energy in GeV.
Determining the values of θ and Δm^2 are the ultimate goals of the MINOS experiment.

4 MINOS

MINOS stands for the Main Injector Neutrino Oscillation Search. It is what is known as a long baseline experiment owing to the large distance over which the neutrinos travel from the artificial source to the final detector. A beam of muon neutrinos will be made at the main injector at Fermilab, Illinois and shot 730km through the earth to Soudan Mine in Minnesota (See Figure 1). The beam is sampled at both ends by the 'Near' and 'Far' detectors. Differences in the neutrino event characteristics and rate yield the physics data we require.

The beam has three available settings such that the peak of the neutrino energies at the Far Detector are 3, 7 and 15 GeV. With the present baseline length, this allows limits on the neutrino oscillation parameters to be determined around the approximate values of $sin^2\theta \sim 1$ and $\Delta m^2 > 10^{-3} eV^2$. This can be done by studying the ratios of weak neutral-current (NC) interactions to weak charged-current (CC) interactions. Weak interactions of muon neutrinos produce muons in the detector which have a very characteristic 'long track' signature. Almost all other interactions produce short 'shower-like' events. So, simply put, if the numbers of long tracks seen decreases between the Near Detector and Far Detector (for a normalised flux) the numbers of muon neutrinos present must have decreased. And this means they may have oscillated from one type to another. The ratio:

$$\frac{\left(\frac{NC}{CC}\right)_{Near}}{\left(\frac{NC}{CC}\right)_{Far}}$$

is a particularly useful measurement since the ratio normalises the flux and eliminates systematic errors. In addition, it is doubly sensitive to oscillations since $\nu_\mu \rightarrow \nu_e$ or ν_τ decreases CC and also increases NC. The lowest beam energy setting is most sensitive to oscillations at a distance of 730km but unfortunately this is below the tau lepton production threshold. Hence we can detect the disappearance of muon neutrinos but not the appearance of tau neutrinos.

4.1 The Far Detector

The Far Detector is currently under construction 715m underground in a disused iron mine in Soudan, Minnesota. It is effectively a magnetised tracking calorimeter using inch thick steel sections and solid scintillating plastic. The steel is organised into 8m wide octagons and each is coupled to 192 strips of 4 x 1 cm scintillator to form a plane (See Figure 2). A small air gap separates each of the 248 planes of 'Super-module 1'. The detector will comprise 2 supermodules - the second having approximately the same number of planes. In total the detector will be over 31m long and weigh 5.4 ktons. In addition each supermodule will have a 15 kAmp-turn coil running through the middle to generate a 1.5 Tesla magnetic field within the steel. This allows the momentum of muons to be determined, by measuring their curvature in the field.

The scintillator strips are read out at both ends by wavelength shifting optical fibres to Hamamatsu M-16 multi-anode photomultiplier tubes (PMT). Each pixel of the PMT receives the signal from 8 scintillator strips. These strips are arranged in such a way that the signal can be uniquely resolved from the double-ended readout. Successive planes have strip orientations rotated through 90 degrees, creating a pseudo-3D detector readout.

Figure 2: The North Face of the Far Detector (Plane 177)

4.2 The Near Detector

The Near Detector's function is to determine the characteristics of the beam just after the neutrinos have been created, before any oscillations have occurred. It is designed to be as similar to the Far Detector as possible so that an unbiased comparison can be made of data from the two detectors. However, it is impossible to make them identical due to the differing neutrino energy spectra and event rates between them.

The Near Detector is slightly scaled down, 280 planes in the shape of an elongated octagon 3.8m high by 4.8m wide (See Figure 3). The beam focus is offset from the centre to prevent neutrino events occurring in the coil hole, whilst saving on scintillator, steel etc. This also means that only a section of each of the first 120 planes requires instrumentation.

In addition the electronic systems are faster, allowing them to handle the much higher event rate expected at the Near Detector.

Only one in every five of the last 160 planes is fully instrumented as the maximum resolution available is not required. They have a complete scintillator layer since multiple Coulomb scattering can spread muons a large distance from the beam centre.

The magnetic field is the same in both detectors.

Figure 3: The Near Detector

4.3 Calibration and the Calibration Detector

Both the Near and Far Detectors need accurate calibration in order that the raw electronic output can be converted into meaningful data.

As charged particles travel through the scintillating plastic strips, light is emitted. Small differences in the fluor density and imperfections in the plastic mean that the strips do not all respond in exactly the same way for a given stimulus. By exposing the strips to a 'standard candle', these differences can be identified and compensated for. In the MINOS experiment, this is done using natural, high energy muons that arise from cosmic rays. As they pass through the detector, they deposit a fixed amount of energy in each of the strips they cross. Over time, a map of the strip responses can be compiled, in relative muon energy units (MEU).

The light that charged particles produce is affected in a number of ways before it can be read out by the PMTs. The transmission at the optical surfaces, the efficiency of the wavelength shifting fibres and the attenuation the light experiences as it travels along the fibres must be compensated for. The PMTs work by absorbing light on a photocathode which emits electrons. These electrons are accelerated by high voltage towards an anode via 12 dynode stages at each of which the number of electrons is multiplied by an avalanche effect. At the anode, the total charge is collected and an amplified electronic signal produced. Therefore the quantum efficiency of the photocathodes and the intrinsic gain of the devices must be taken

into account in the calibration of the system. To remove these effects, a specially designed light injection system is used. This works by inputting a known quantity of light into the detector thereby simulating a particle causing emission of light from the scintillator. Ultra-bright blue LEDs are used to generate the light; the wavelength shifting fibres modify the LEDs' spectra to be similar to that from the scintillator and also prevent the scintillator re-absorbing the light it emits. Special PIN diodes are used to independently measure the quantity of light from the LEDs. These produce a more linear charge response to light than the PMTs, but do not function as well at the low light levels required. Thus a quantity of charge that is linear with light and therefore MEU are obtained.

Lastly, systematic effects in the readout electronics and charge digitisation must be calibrated out. This is done by injecting a known quantity of charge into the system to measure the response. The input charge is measured using a digital potentiometer which is very linear over the region required. The final data output from the Front-End electronics is a unit known as ADCs (from Analogue to Digital Converters) The complete calibration system results in ADCs being linearly proportional to MEU.

Unfortunately, MEU at the Near Detector are not directly comparable to those at the Far Detector since the muon energy ranges are different. The Far Detector is shielded by rock equivalent to water of a depth of 2100m. Only muons around 100 GeV can penetrate this far. The Near Detector is much closer to the surface and so the muons are just a few GeV. It is possible to make a comparison using muons that stop within the two detectors. The energy of these muons can be determined to a reasonable accuracy by measuring the distance they are able to travel through the detector and comparing this with Monte Carlo studies.

Stopping muons provide a good Near to Far calibration. However what is really required is a measure of the absolute energy of the particles interacting in the detectors. To do this, the interactions of particles of known energies must be observed. In order to accomplish this, a third detector has been built: the Calibration Detector.

The Calibration detector has been constructed and assembled in at CERN, Switzerland. It is a scaled down version of the other detectors consisting of 60 1m x 1m planes (See Figure 4). It has no magnetic field and reads out via clear fibres on one side and green on the other in order to simulate the attenuation suffered by the light through the much longer fibres at the main detectors. Each fibre goes to an individual PMT pixel, so no strip de-muxing is required. The calibration detector has run with electronics identical to those used at the Far Detector and will run with Near Detector electronics soon for comparison. The Calibration Detector runs in the T11 and T9 test beams at CERN where pions, protons, electrons and muons of known energies are incident upon it. In addition to the instruments available to the main detectors, CalDet has time of flight and Cerenkov apparatus which together with Monte Carlo studies allow the responses of the different particles at different

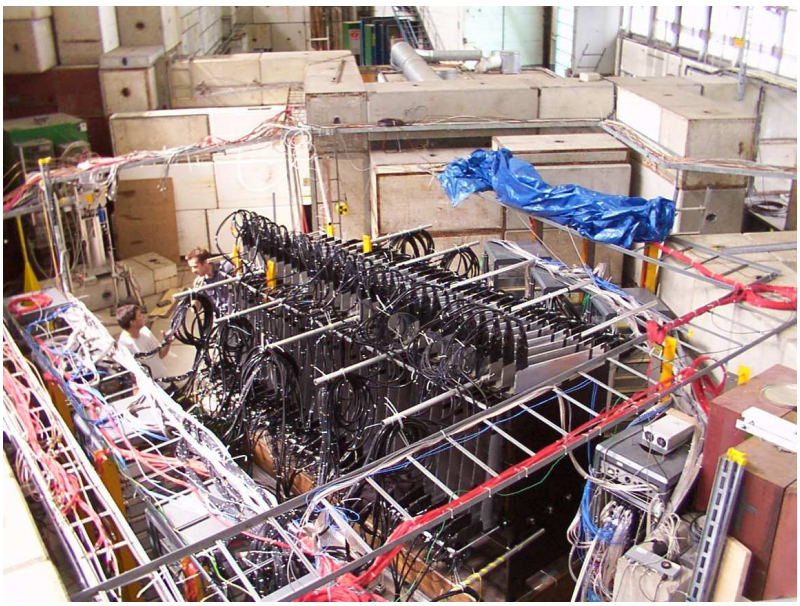

Figure 4: CalDet in T11

energies to be separated. By carrying this calibration to the main detectors, the visible energy of all the interactions seen can be determined.

5 Monte Carlo

Monte Carlo is a system used widely in particle physics today. It it simply a computer simulation of a detector into which specific particle interactions can be programmed to be studied. Its main advantage is that huge numbers of particles can be simulated rapidly, generating good statistics. By putting cuts on the outputs it is possible to focus on the problem regions, for example the few pions in the tail of a range distribution that look identical to muons. It is by using these simulations that techniques can be developed for identifying different particles in the detector.

The simulation program used was Geant 3.21. It incorporates a number of physical effects making it a very accurate simulation of the Calibration Detector. These effects include Rayleigh Scattering, Gamma induced fission, pair production, delta ray generation and Bremsstrahlung. Optical effects such as the wavelength shifting fibre light trapping efficiency and Birk's scintillator saturation effect are present. And real detector features include the double ended readout, green and clear fibre readout, a 1% spreading of initial particle momenta and a full simulation of the PMT including all 12 dynode stages.

Geant runs on parameters set using FORTRAN code. There is a more contempo-

rary program using C++ which has in fact been designed for the MINOS geometry, called gMINOS. This is fairly new however and still under development.

6 Muon de/dx and a study of the T11 beam

Checking real data against Monte Carlo simulations is an important part of the experiment because it helps to verify that all the physical effects present in the detector are understood.

It is essential to be able to model muons paths through the detector as part of the overall calibration. A simple aspect of this is to study the range of muons in the detector. This is simply the distance a muon travels before stopping. At the CalDet, the vast majority of muons come from the beam and hit the first plane, so it is equivalent to refer to the range as the 'last plane hit'. 6000 muons were generated in the Monte Carlo simulation for each of the energies 0.8, 1, 1.4, 1.6 and 2 GeV. An algorithm was written to track their progress through the detector and return the last plane hit. The results were collated and plotted and a Gaussian fit to the distribution to produce a mean. An example of this is given in Figure 5. Figure 6 shows all of the results.

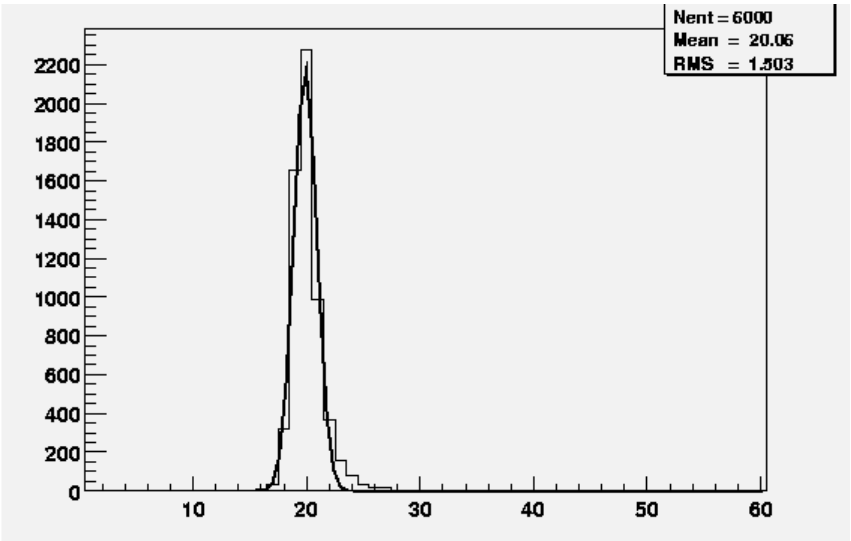

Figure 5: 0.8 Gev Last Plane Hit

By extracting the means and plotting them separately, a straight line can be fitted. This process was done for positive and negative muons (Figure 7). On the scale of the graph, the positive and negative curves cannot be separated; the difference is about 0.75%. The graph to the right shows the differences between the

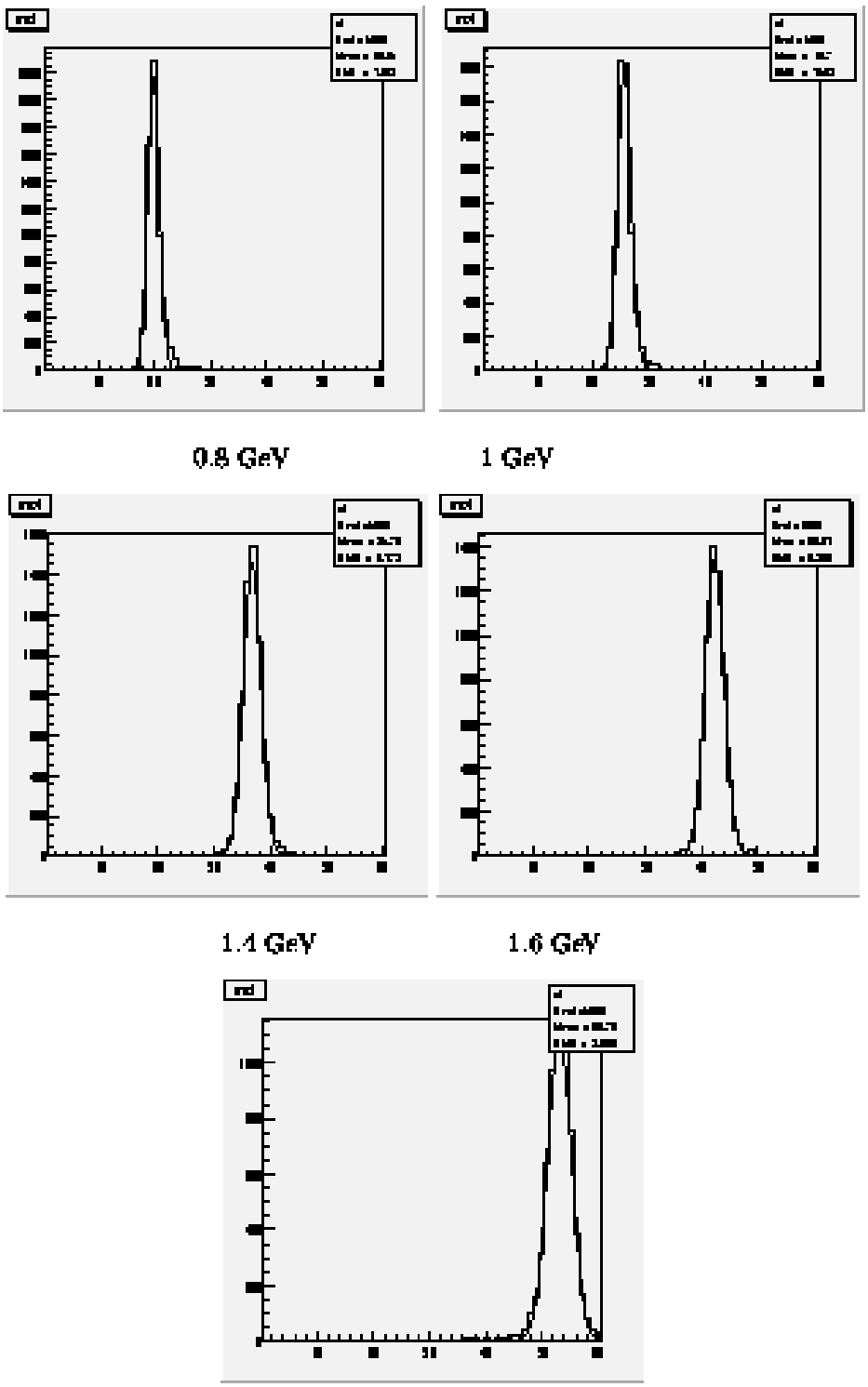

Figure 6: Gaussian fitted to Last Plane Hit from Monte Carlo data at various energies

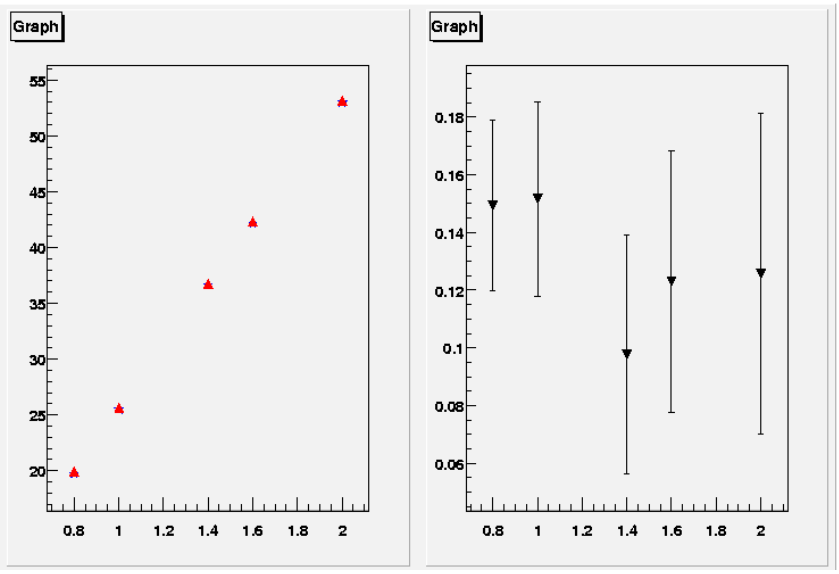

Figure 7: Left: Last Plane Hit against Muon Energy, Right: Differences of Positive and Negative Muons

two types of muons at each point. It shows that the positive muons consistently loose slightly more energy than the negative ones; this effect is expected from theory.

This simple study can be extended by tracking the muons more closely and looking to see how much energy they deposit in each of the strips they pass through. Figure 8 shows this for 2 GeV Monte Carlo muons with clear fibre readout. As the muon looses energy, it eventually passes below a threshold. At this point the remainder of the energy is deposited in a relatively small region, sometimes in a shower-like event.

The next step is to compare this to real data. A number of modifications have to be applied since the real data has a number of added environmental effects which have to be taken into account. For data to pass the selection process identifying it as a 'real muon', there must be at least 16 hits anywhere in the detector and always a clear and green signal from each hit. This is to remove spurious noise hits without disrupting the muon track. Only muon tracks that make an angle of less than 10 degrees to the beamline are accepted to remove the possibility of the muon having a source other than the beam pipe (since it has an unknown energy). There must also be less than 3 hits in a given plane to remove 'muon-like' pions from the sample. A minimum energy deposit is required to register a hit as genuine. This is known as the sparsification threshold and is set to a third of a photoelectron which is about 30 ADCs. These cuts are also applied to the Monte Carlo to make a fair comparison. The results are shown in Figure 9.

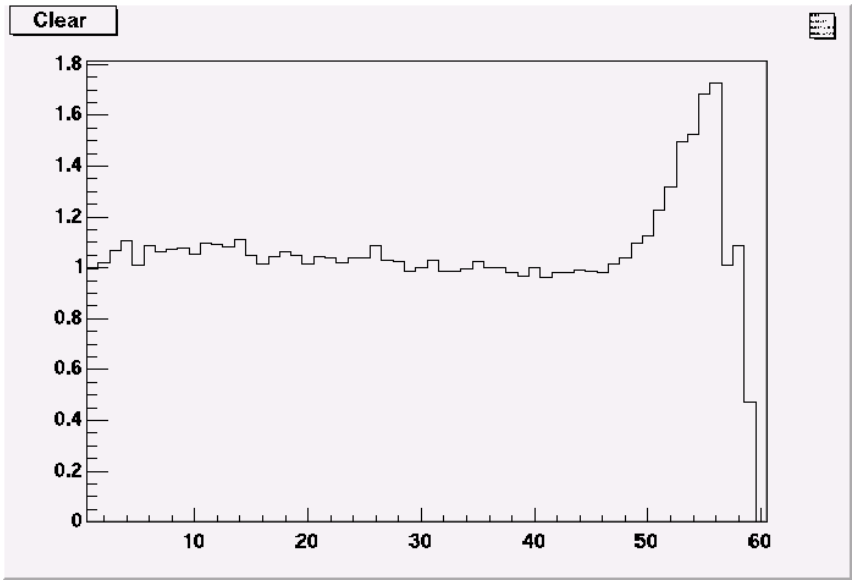

Figure 8: The rate of energy loss of a muon as it travels through the detector, normalised to the energy deposited in the first plane

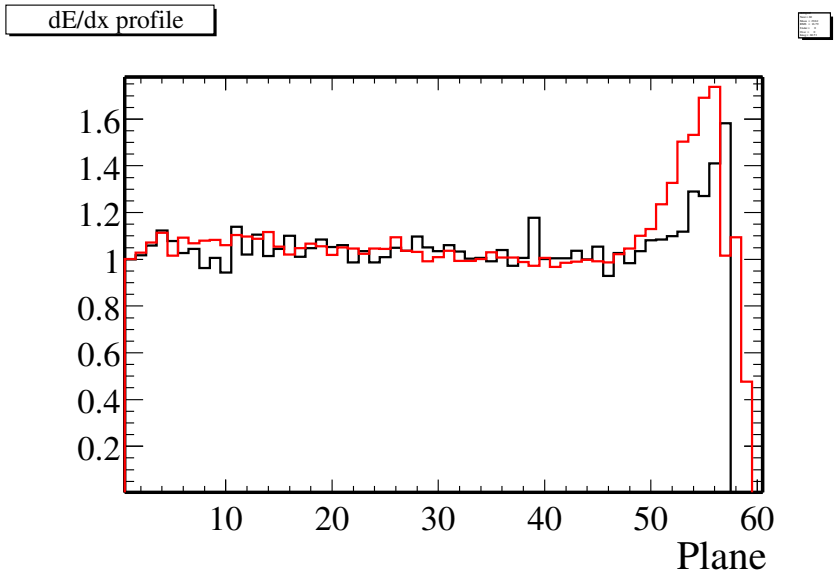

Figure 9: The rate of energy losses of muons. Monte Carlo is shown in red and real data is black

The data agrees with the Monte Carlo well for the first 40 planes or so. The spread of the data is reduced around the last plane hit peak because only muons that stop in planes 54, 55 and 56 are allowed. This cut is necessary since the all the muons in the Monte Carlo sample have 2 GeV but in the real data this is the energy maximum and there are in fact some with lower energy present. These stop sooner and pollute the low energy tail of the distribution.

However, the most important feature of this comparison is the fact that the peaks of the distributions do not coincide. This shows that there is a discrepancy between the last plane hit predicted in the Monte Carlo and that seen in the data.

By repeating the process of finding the last plane hit that was done before, but using real data, a better value for the beam energy is found (See Figure 10) at 2.05 GeV, a difference of 2.5%. This suggests that the focussing magnets have deviated from their nominal position causing a slight shift upwards in energy.

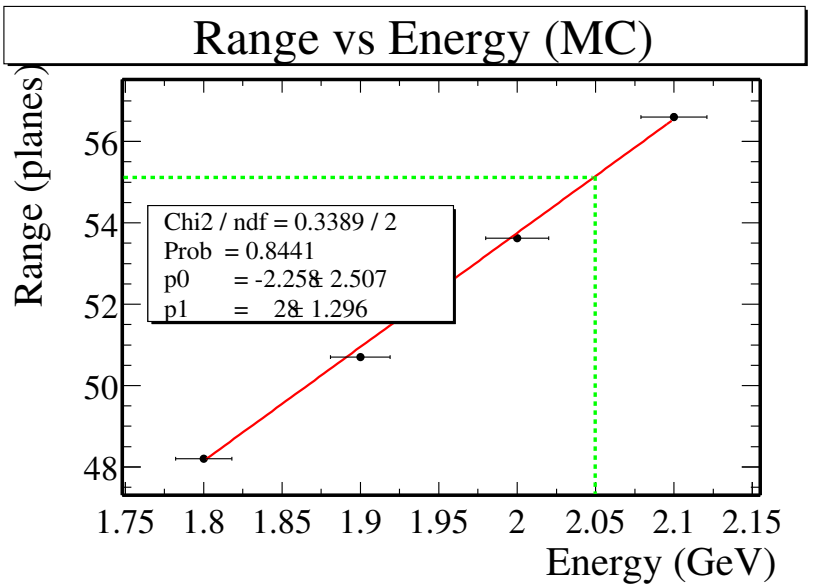

Figure 10: The rate of energy losses of muons. Monte Carlo is shown in red and real data is black

Even at this new energy, there is still a significant discrepancy between Monte Carlo and data. At 2.05 GeV, virtually no muons leave the back of the detector (although they come pretty close, see Figure 11) whereas a large quantity appear to in the real data (Figure 12). The low energy tail in the real data is mainly low energy muons and 'muon-like' pions.

A plot of de/dx also does not quite look correct (Figure 13). The real data is normalised using 3 GeV muons that pass all the way through the detector to remove scintillator effects.

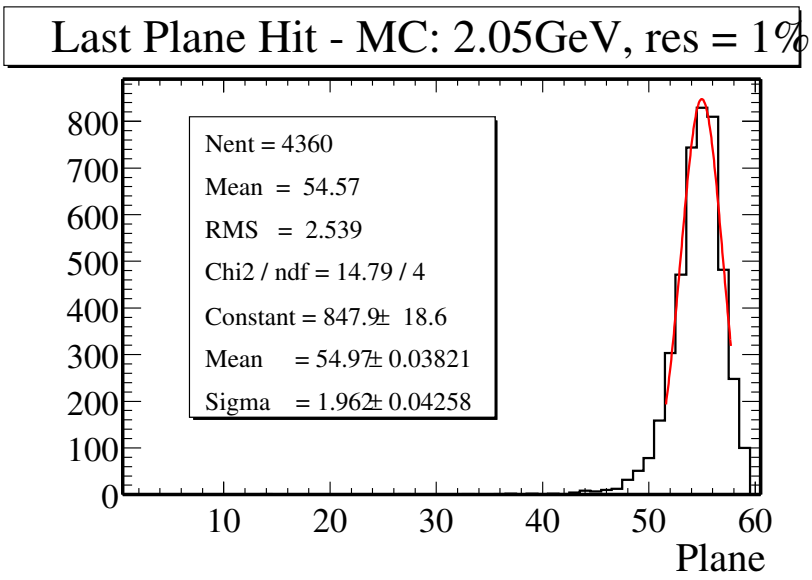

Figure 11: Monte Carlo Last Plane Hit at 2.05 GeV

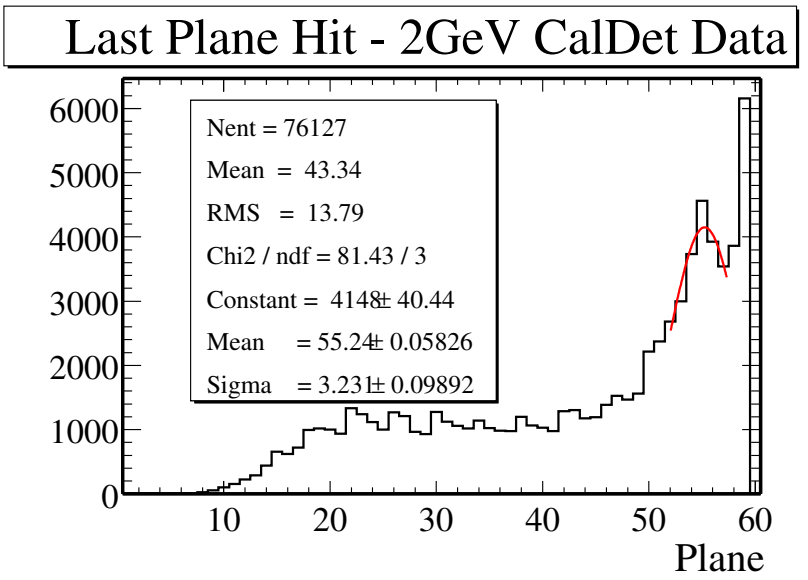

Figure 12: Real Data Last Plane Hit at '2' GeV

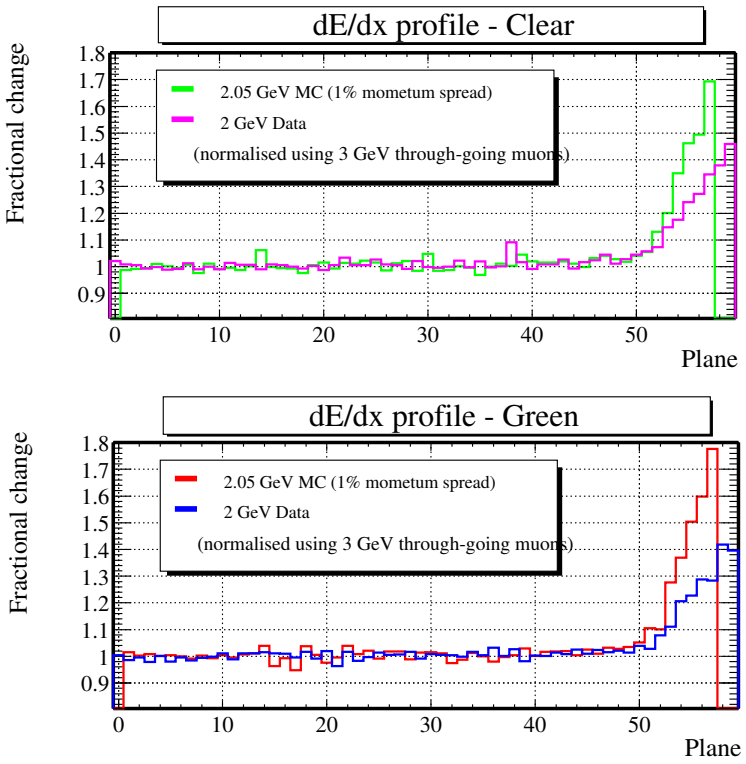

Figure 13: de/dx real and Monte Carlo

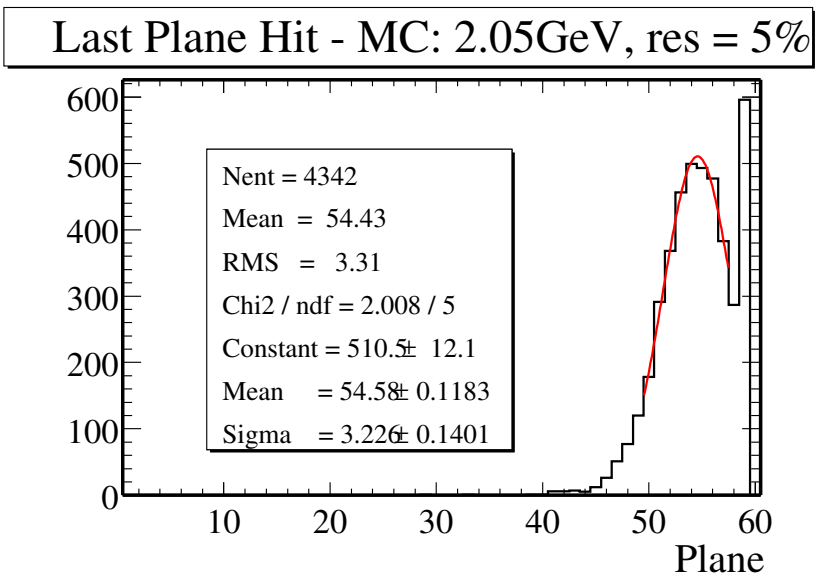

Figure 14: Monte Carlo Last Plane Hit at 2.05 GeV with 5% momentum spread

To attempt to compensate for this, the parameters in the Monte Carlo were adjusted again. This time the spread of the momenta of the particles produced was increased from 1.5% to 5%. This produces a distribution (Figure 14) that is much closer to the observed data (Figure 12).

And the resulting de/dx plot is very close to the data (See Figure 15).

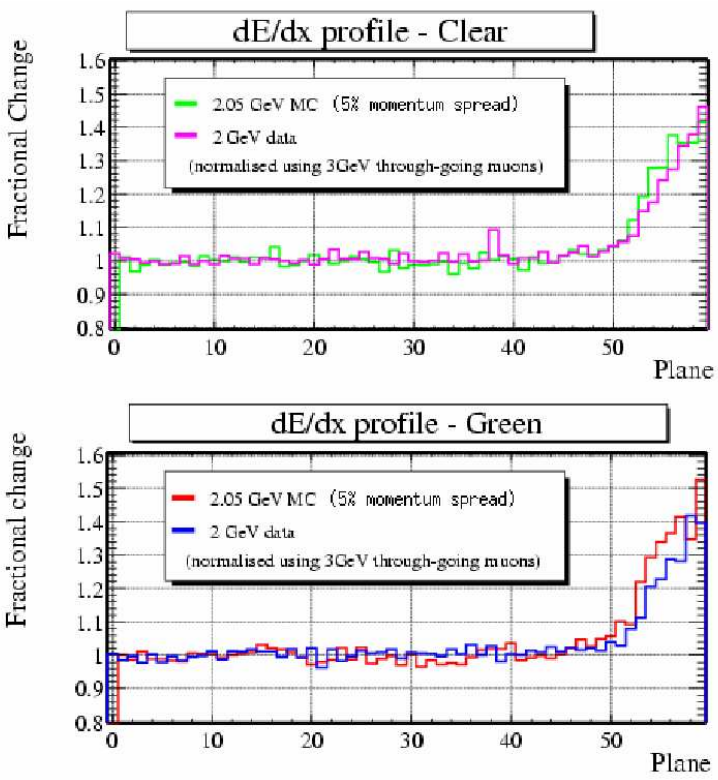

Figure 15: de/dx Real and Monte Carlo using 2.05 GeV muons with a 5% momentum spread

So it has been established that the beam parameters appear not to meet the stated specifications. The next step is to pin down exactly the magnitude of the deviations seen. Using Monte Carlo at a number of different momenta (See Appendix B) it is possible to fit a polynomial to the widths of the resulting distributions. The errors on the graphs are given from the fit (See Figure 16). This was done at 1.4 GeV to remove any possible edge effects seen before.

This compares favourably to the real data. The best fit value of the momentum spread if 4.6%. The gaussian is only fitted to part of the graph to remove lower energy muons.

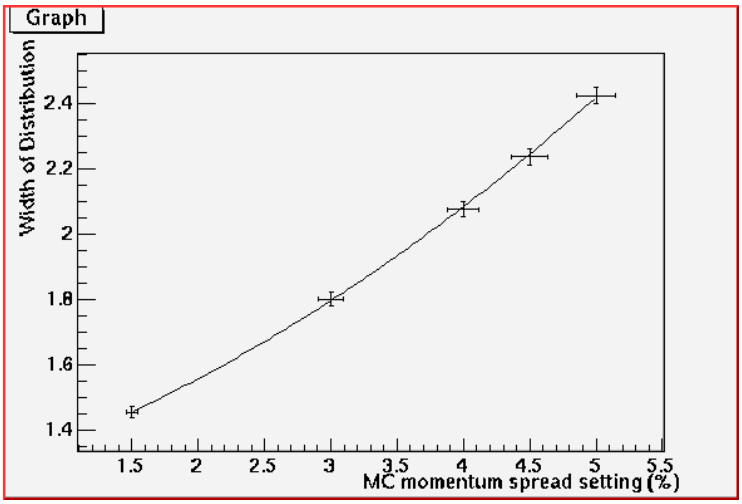

Figure 16: Fit to the widths of the varying momentum distributions

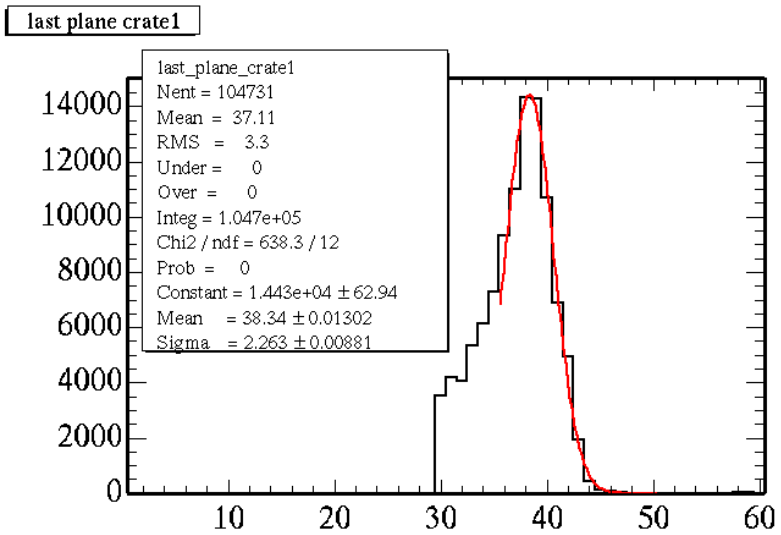

Figure 17: Real Data at 1.4 GeV

A similar procedure was applied to a range of energies around 1.4 GeV (Figure 17). A straight line fit to the Monte Carlo data, fixed at a momentum of 4.6% yielded a best fit of 1.454 GeV, a discrepancy of 3.86%. This produces a final result which matches the data well (Figure 18).

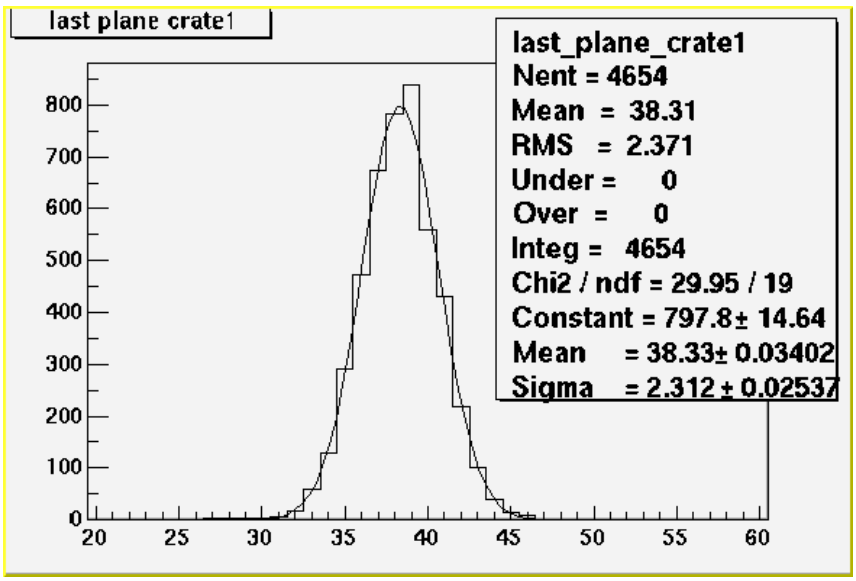

Figure 18: Finished Monte Carlo simulation: 1.454 GeV and 4.6% momentum spread

7 Conclusions and Further Analyses

The conclusion reached is that the Monte Carlo modelling of de/dx of muons through the calibration detector is fairly accurate. But not at the specifications of the T11 beam. In fact the energy of the beam seems to deviate from the defined value and there is a wider spread of particle momenta than expected. The alignment of the focusing magnets may be partly at fault; there also may be some factor resulting from particles interacting with the beam pipe just downstream of the magnets.

It may be interesting to see how this effect changes with energy. At 1.4 GeV there was a 3.8% discrepancy in energy, but at 2 GeV it was only 2.5%. This may just be a statistical effect however.

The information derived from these studies can eventually be compared to similar data from cosmic ray muons, leading to a conversion system from muon energy deposits to visible energy that is applicable to both the Near and Far detectors.

8 References

Special thanks to Chris Smith and Ruben Saakyan for their help.

1) An LED calibration system for the MINOS long baseline neutrino experiment, P.Adamson, March 2001

2) Testing the dynamics of ν_μ to ν_τ conversion, A. M. Gago, E. M. Santos, W. J. C. Teves, R. Zukanovich Funchal

3) The Light Production of the MINOS Mini Calibration Module, C. Smith, June 2000

4) The MINOS light injection spectra at low light levels, R. Nichol, June 2001

5) The MINOS Long Baseline Neutrino Oscillation Experiment, Minos collaboration @ UCL, Oxford, RAL, Sussex, March 1999

9 Appendices

9.1 Appendix Index

9.2 Appendix A: Last Plane Hit at Varying Energies

Figure 19 - Last Plane Hit of 1 GeV muons
Figure 20 - Last Plane Hit of 1.4 GeV muons
Figure 21 - Last Plane Hit of 1.6 GeV muons
Figure 22 - Last Plane Hit of 2 GeV muons

9.3 Appendix B: Fits to Gaussian widths from varying momentum Monte Carlo

Figure 23 - Monte Carlo Last Plane Hit at 1.4 GeV with varying momentum spreads

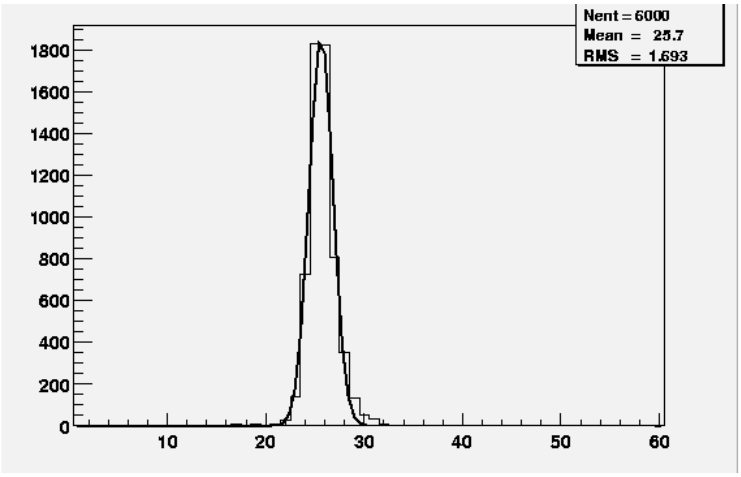

Figure 19: A: 1 Gev Last Plane Hit

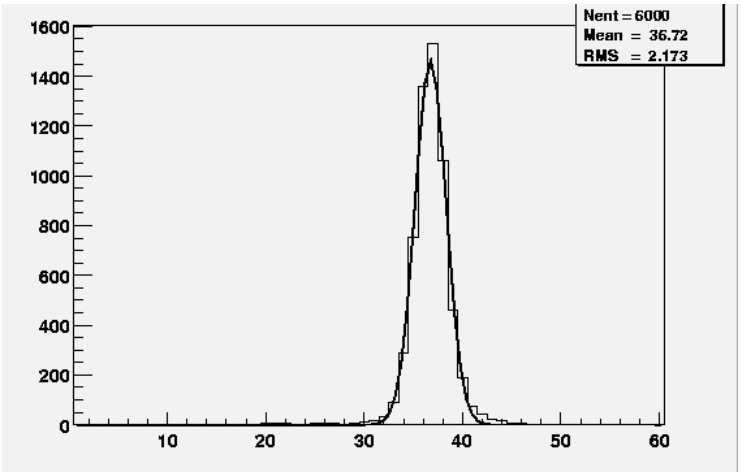

Figure 20: A: 1.4 Gev Last Plane Hit

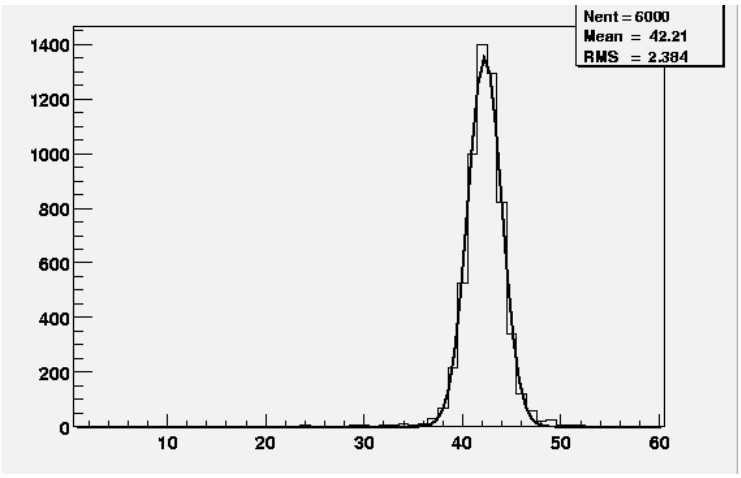

Figure 21: A: 1.6 Gev Last Plane Hit

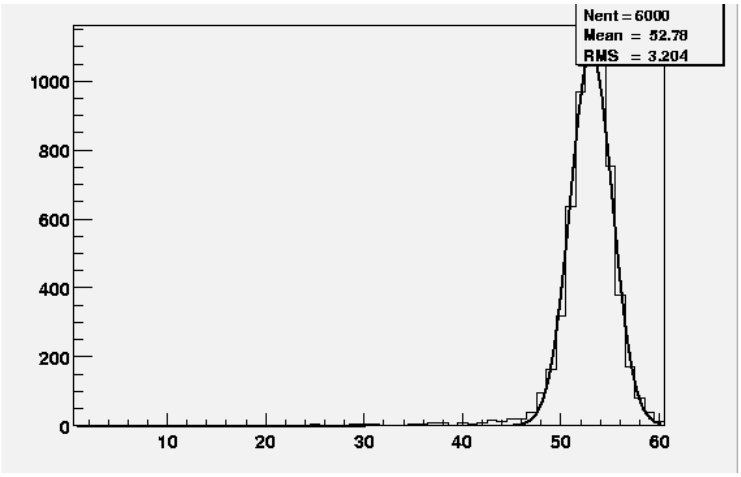

Figure 22: A: 2 Gev Last Plane Hit

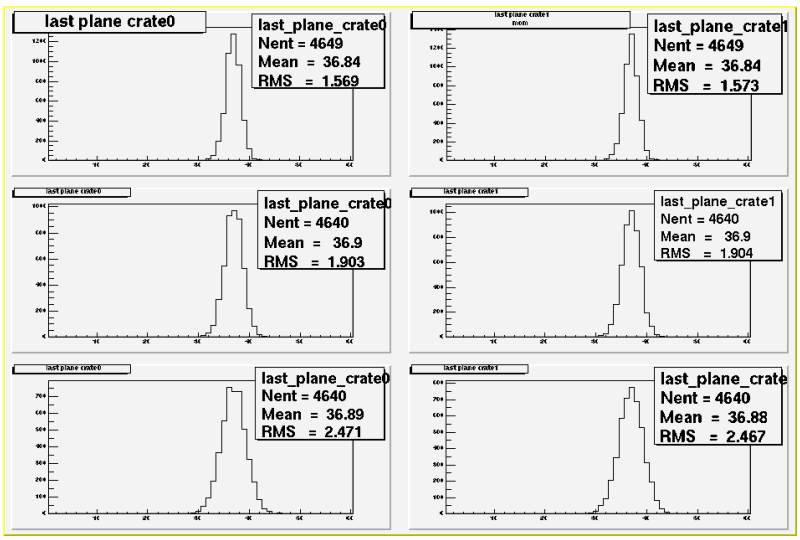

Figure 23: B: Left: 1, 3, 5 % spread Crate 0, Right: 1, 3, 5 % spread Crate 1